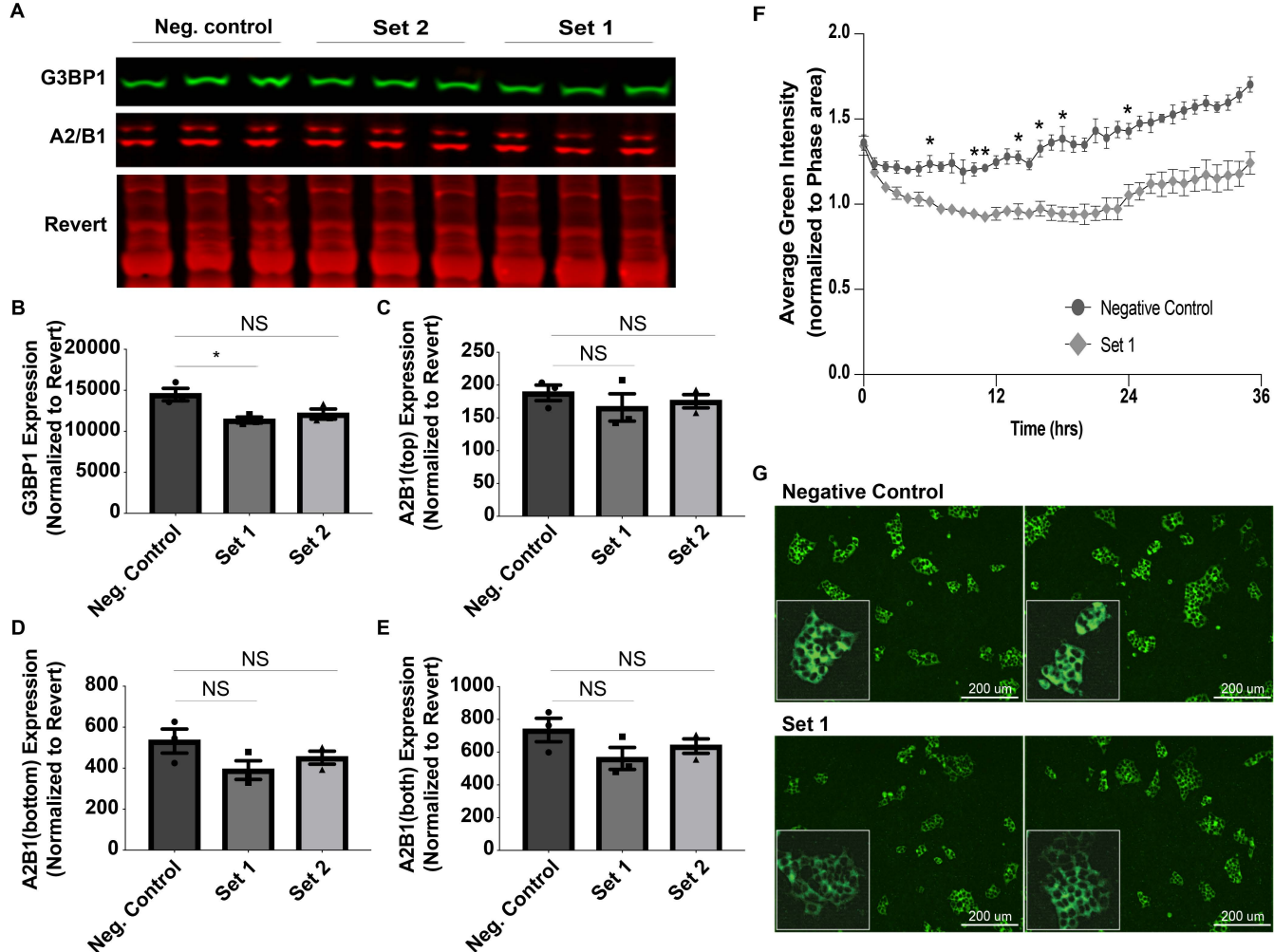**Supplemental Figure 1. Average size distribution curves of individual CSF EV samples.** EVs were isolated from CSF collected from HD and control patients by membrane affinity column centrifugation and resuspended in PBS (N= 5 HD, 5 control). Isolated EVs were analyzed in triplicate by fluorescent nanoparticle tracking analysis. Red error bars indicate ±1 SEM.

Supplemental Figure 2. Downregulation of G3BP1 protein levels by overexpression of synthetic miRNAs in 293T cells. A) Western blot of G3BP1, hnRNPA2/B1 (A2/B1), and total protein (Revert). **B)** G3BP1 protein expression normalized to total protein is significantly lower in Set 1 miRNA cocktail treated cells compared to the negative control (One-way ANOVA, Dunnett's multiple comparison test, *=P=0.019), but not Set 2 miRNA cocktail treated cells. **C-E)** hnRNPA2/B1 expression of individual isoforms ('top' vs. 'bottom') and both isoforms together normalized to total protein is also not significantly different among treatment groups. **F)** Graph depicting the average G3BP1 signal across time from Set 1 microRNA mimic cocktail or negative control transfected 293T-G3BP1-GFP cells measured by Incucyte S3. Y-axis depicts the average intensity value per image at a particular time point. Repeated measures two-way ANOVA with Bonferroni's multiple comparison test was performed (*=P<0.05). Each data point represents averages from 4 images per well, and 4 wells per condition. **G)** Representative images that were used for graph generation at the 25hr timepoint show lower G3BP-GFP fluorescence signal from Set 1 treated cells (bottom) compared to negative control treated cells (top).
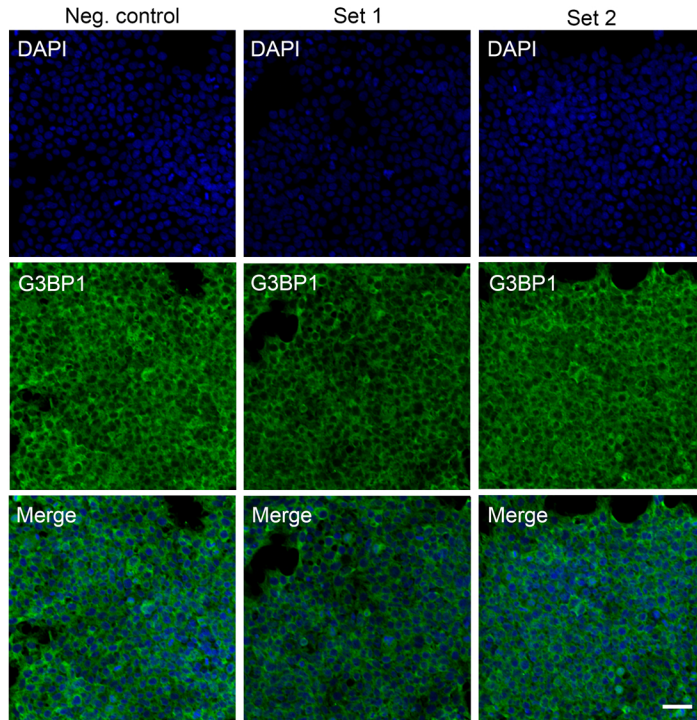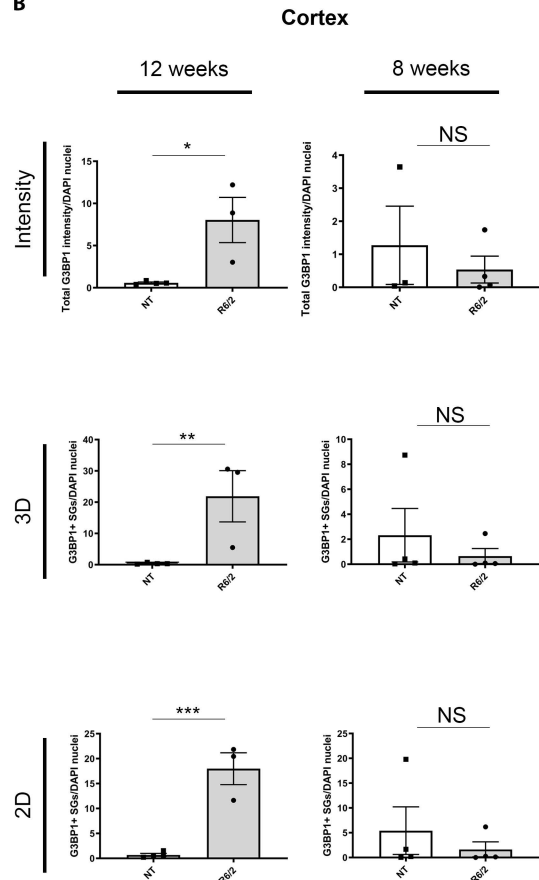
Supplemental Figure 3. 293T cell single channel images from Figure 4 (unstressed conditon): G3BP1-mediated stress granule induction is regulated by miRNAs in 293T cells treated with sodium arsenite. Cells were transfected with either a negative control miRNA (Neg. control), a 4-miRNA cocktail (Set 1), or a 3-miRNA cocktail (Set 2), (N=3 per condition). Scale bar= 40um.
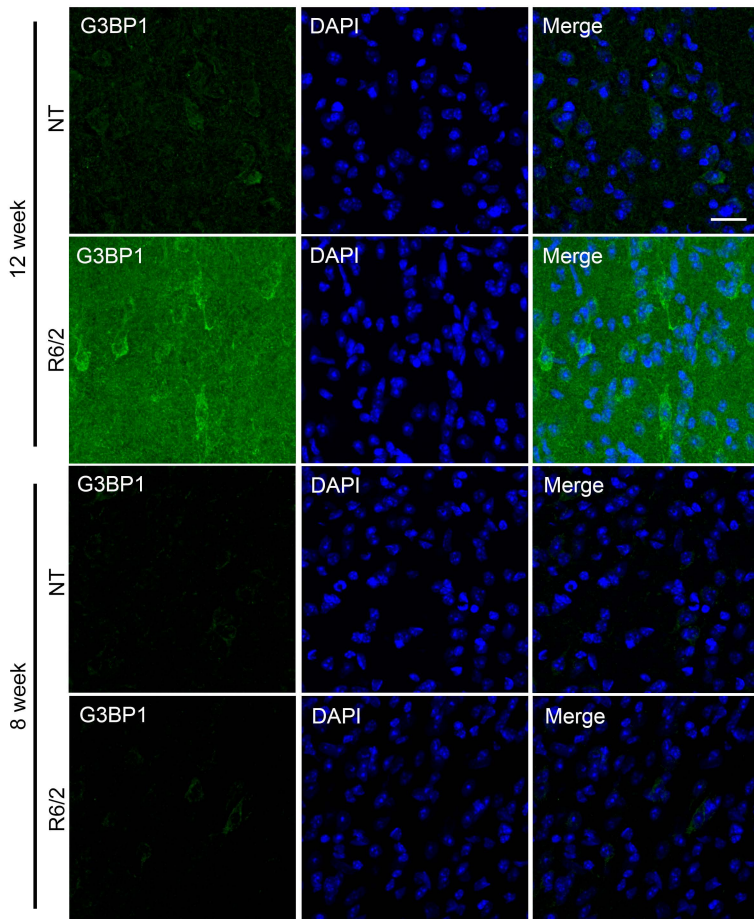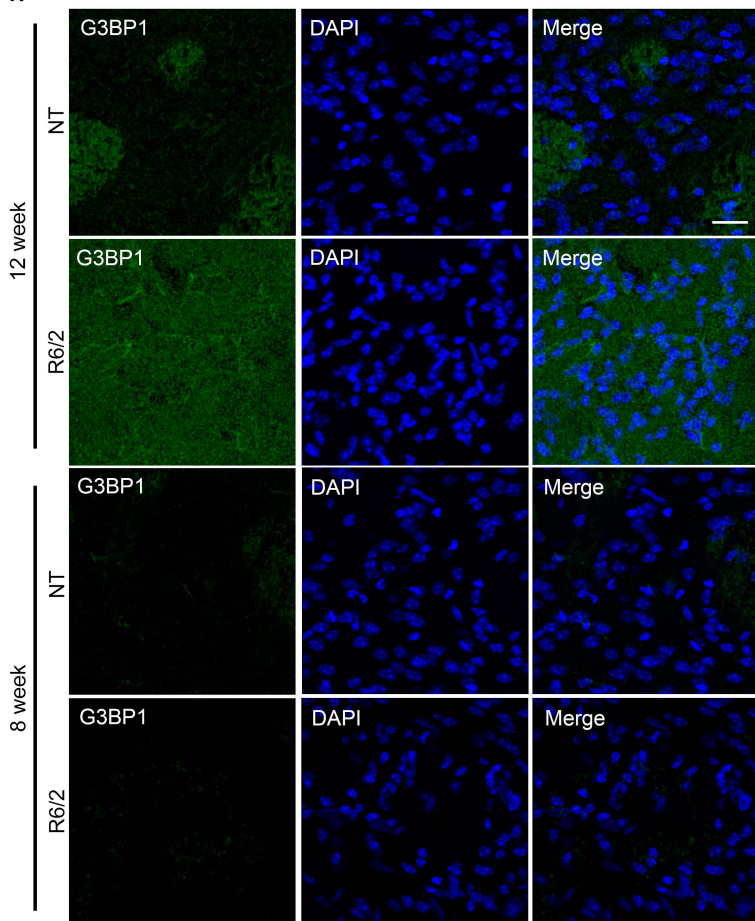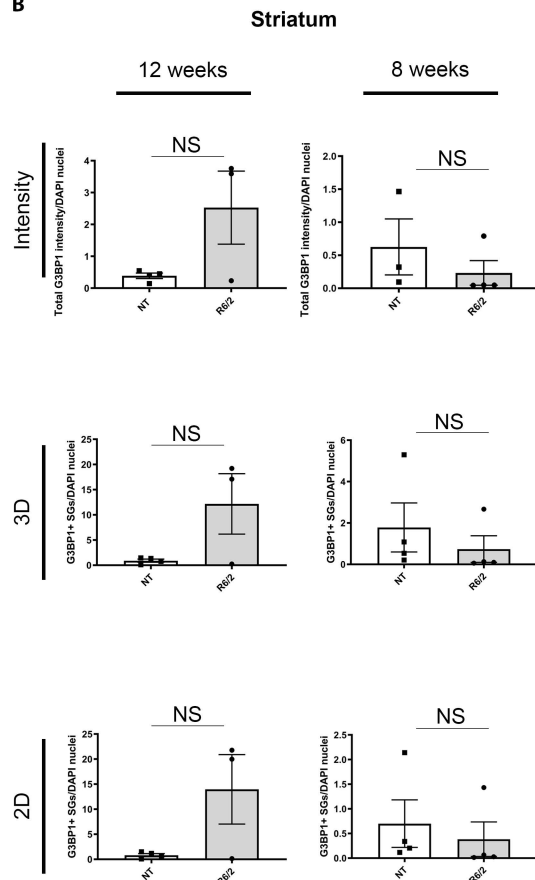
Supplemental Figure 4. G3BP1 granule density analyses in the R6/2 cortex at 8 and 12-week timepoints. A) Representative images of the R6/2 cortex at 12 weeks demonstrate an increase in G3BP1 immunoreactivity compared to the NT cortex. Scale bar =20um. **B)** G3BP1 pathology was assessed by measuring G3BP1 immunoreactivity intensity with CellProfiler, as well as G3BP1 granule density using the Imaris surface tool (3-dimensional granule surface detection) and a previously described CellProfiler protocol (2-dimensional granule detection (39)). G3BP1 immunoreactivity and granule density were significantly higher by all measures in the R6/2 cortex at 12 weeks (Student's t-test, unpaired, two-tailed, *=P=0.0210; **=P=0.0014; ***=P=0.0259), but not at 8 weeks. Analyses were done using four frames per mouse brain (N= 12 weeks: 3 R6/2, 4 NT; 8 weeks: 4 R6/2, 4 NT). G3BP1 intensity and granule counts were normalized to the number of nuclei per frame (DAPI). For the creation of this figure, the gamma setting for the green channel was equally adjusted to 0.5 for all images. All analyses were carried out with the original, unedited images.

Supplemental Figure 5. G3BP1 granule density analyses in the R6/2 striatum at 8 and 12-week timepoints. A) Representative images of the R6/2 and NT striatum. Scale bar =20um. **B)** G3BP1 pathology was assessed by measuring G3BP1 immunoreactivity intensity with CellProfiler, as well as G3BP1 granule density using the Imaris surface tool (3-dimensional granule surface detection) and a previously described CellProfiler protocol (2-dimensional granule detection (39)). No statistically significant differences were detected between R6/2 and NT mice in regards to G3BP1 immunoreactivity or granule density in the striatum, at either the 8- or 12-week timepoint. Analyses were done using four frames per mouse brain (N= 12 weeks: 3 R6/2, 4 NT; 8 weeks: 4 R6/2, 4 NT). G3BP1 intensity and granule counts were normalized to the number of nuclei per frame (DAPI). For the creation of this figure, the gamma setting for the green channel was equally adjusted to 0.5 for all images. All analyses were carried out with the original, unedited images.
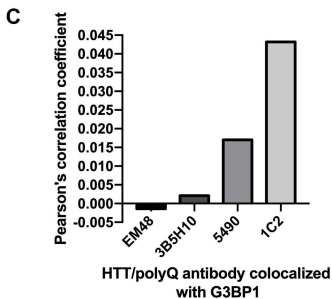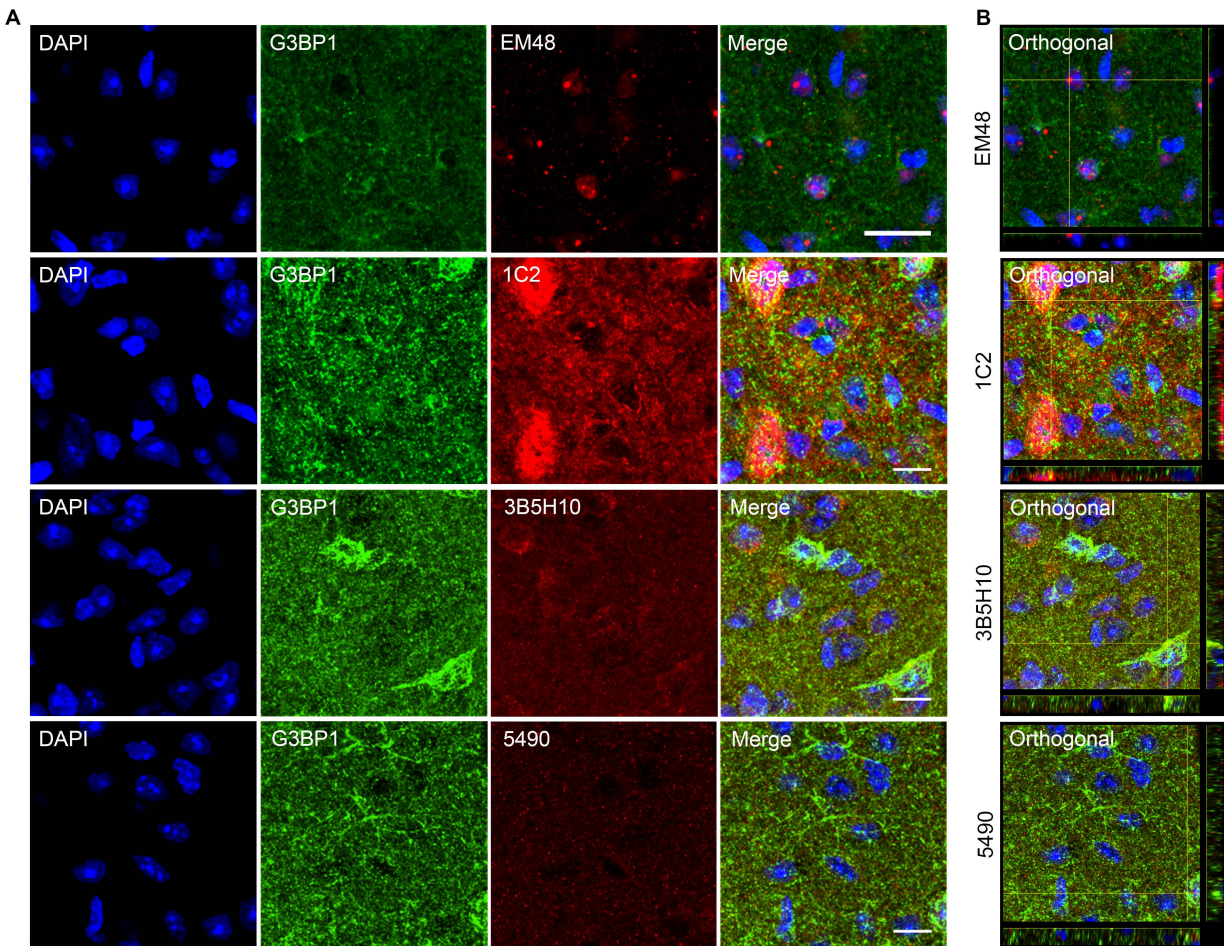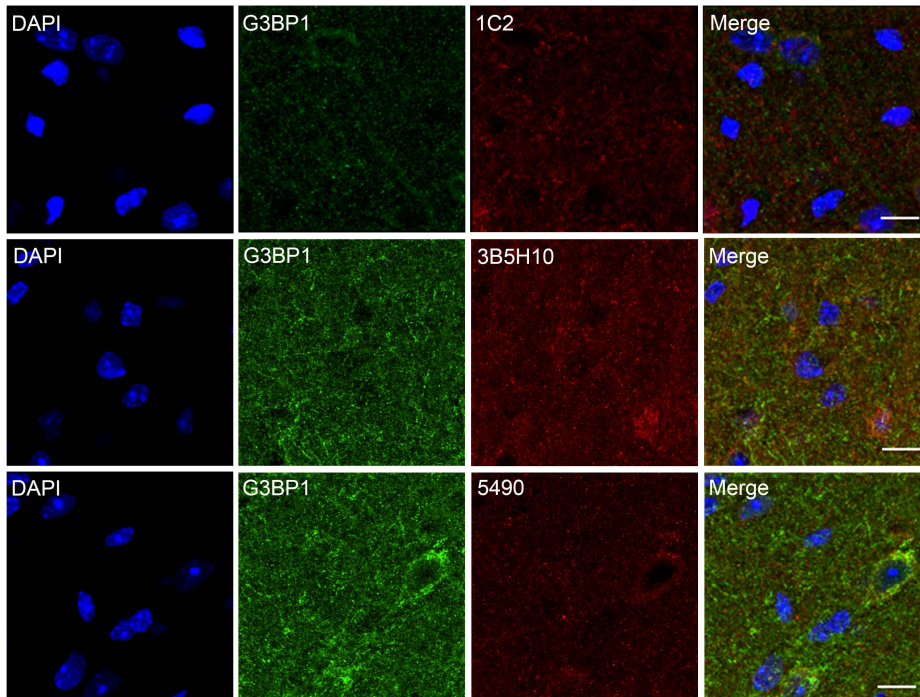
Supplemental Figure 6. G3BP1 granules do not co-localize with EM48-positive nuclear inclusions in the 12-week R6/2 mouse cortex. A) Colocalization of G3BP1 (in green) and HTT/polyQ (in red) was assessed using the antibodies EM48, 1C2, 3B5H10, and 5490. All images shown are maximum intensity projections of 10-slice Z-stacks taken at a thickness of 0.5 um per slice. **B)** Orthogonal views of the maximum intensity projections show modest colocalization of G3BP1 and HTT/polyQ antibodies 1C2, 3B5H10, and 5490, but not EM48. **C)** Pearson's correlation coefficient was calculated for each Z-stack using the Imaris colocalization tool (N=1), with 1C2 having the highest degree of fluorophore colocalization with G3BP1. **D)** Non-transgenic brain stains for comparison. Scale bars= 10 um.

D

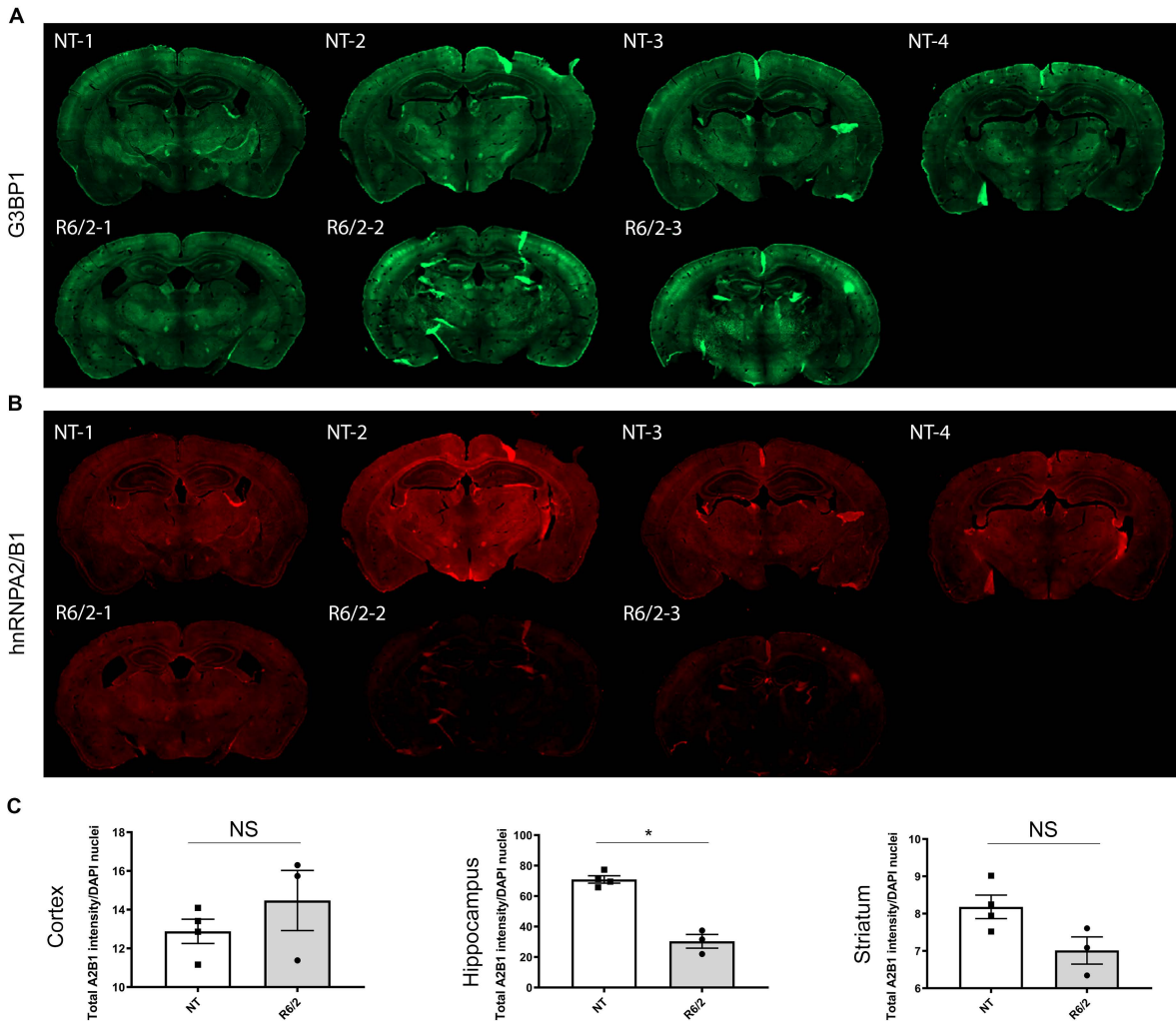| DAPI | G3BP1 | 1C2 | Merge |
| DAPI | G3BP1 | 3B5H10 | Merge |
| DAPI | G3BP1 | 5490 | Merge |

Supplemental Figure 6 (continued). G3BP1 granules do not co-localize with EM48-positive nuclear inclusions in the 12-week R6/2 mouse cortex. D) Non-transgenic brain stains for comparison. Scale bars= 10 um.

Supplemental Figure 7. Comparison of hnRNPA2/B1 and G3BP1 immunoreactivity in the 12-week R6/2 brain. Coronal brain section images of **A)** G3BP1 demonstrate higher G3BP1 immunoreactivity in cortical areas, particularly in R6/2 mice #2 and #3. Conversely, **B)** hnRNPA2/B1 immunoreactivity appears to be lower in the mouse brain sections with highest G3BP1 immunoreactivity. **C)** hnRNPA2B1 immunoreactivity is significantly lower in the hippocampus (Student's t-test, unpaired, two-tailed, *=P=0.0003), but not the cortex or striatum. Immunoreactivity intensity was assessed using CellProfiler and normalized to number of nuclei per frame. Analyses were done using four frames per mouse brain (N= 3 R6/2; 4 NT).
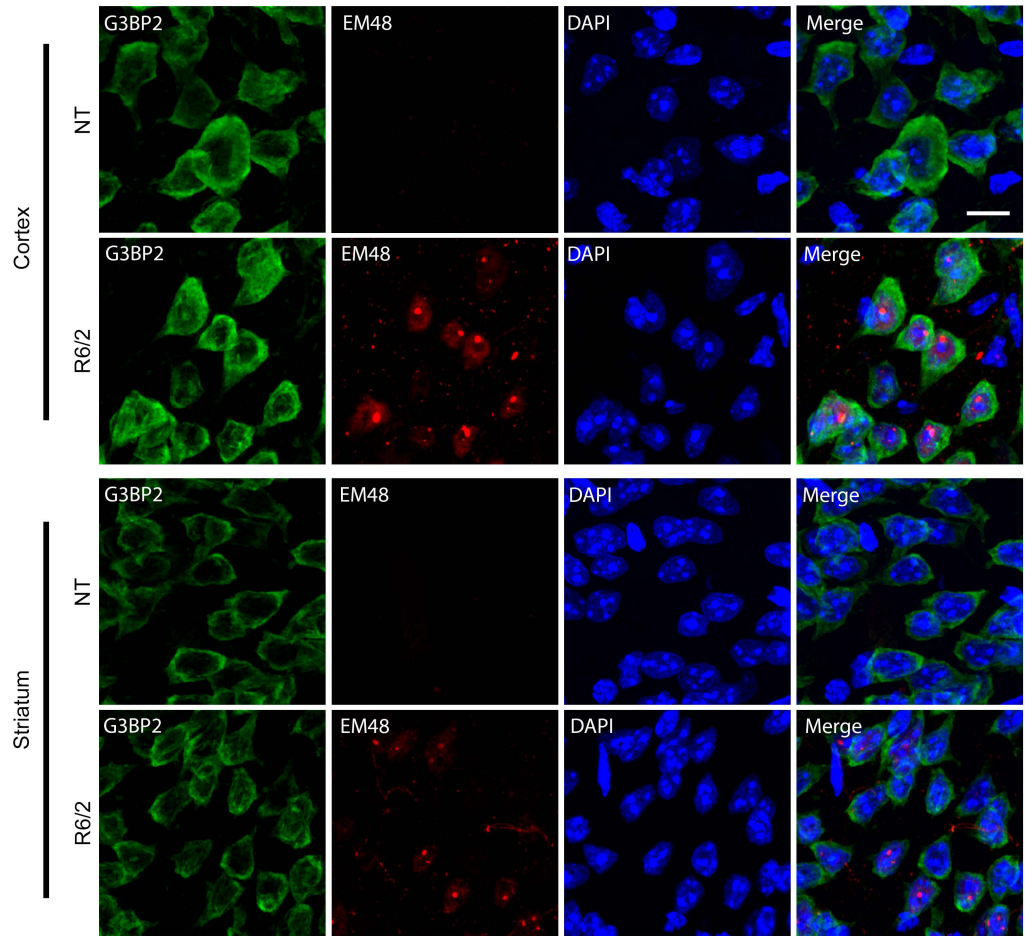
Supplemental Figure 8. G3BP2 granules are not detected in the 12-week R6/2 mouse brain. Immunofluorescence was used to investigate whether the G3BP1 homolog, G3BP2, contributes to pathology in the R6/2 brain. The pattern of G3BP2 immunoreactivity (in green) suggests that, although the majority is localized to the cytoplasm, G3BP2 does not localize to granule-like cytoplasmic structures in the cortex or striatum of either the R6/2 or NT mouse brain. Co-staining with the HTT antibody EM48 (in red) suggests that G3BP2 does not localize to HTT nuclear inclusions. Scale bar= 10um.
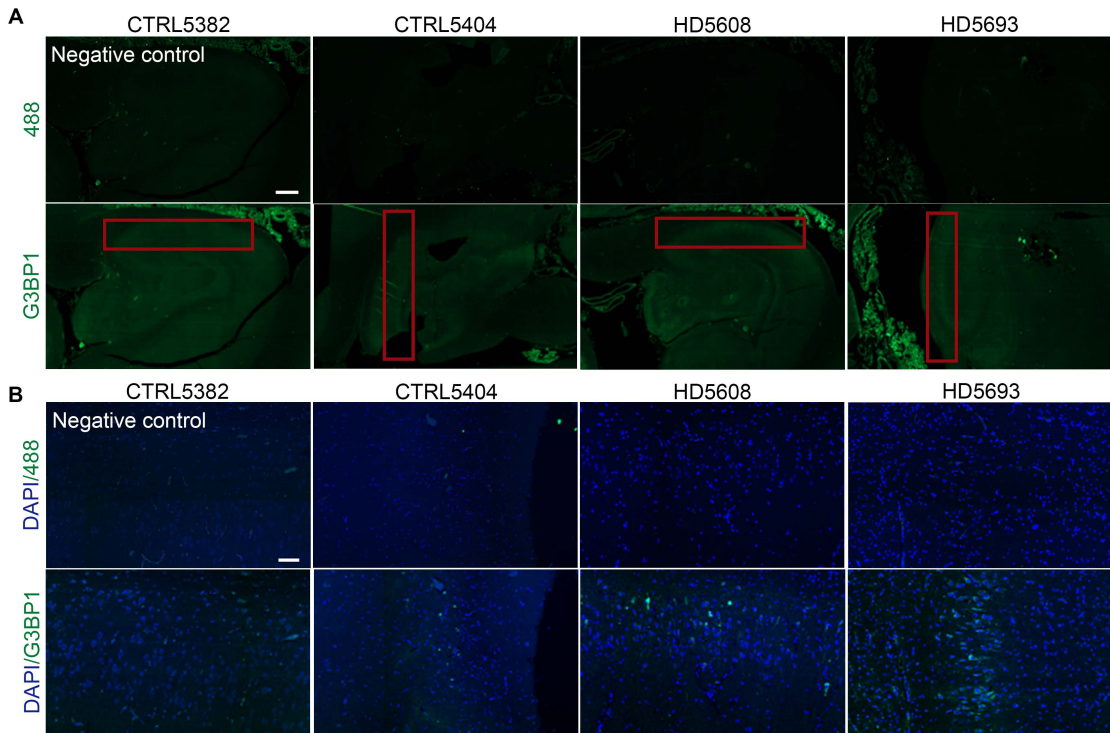
Supplemental Figure 9. G3BP1 immunoreactivity in the hippocampus of HD patients. G3BP1 immunofluorescence of the hippocampal formation in HD (grade 2) and control brains. **A)** Scans of the full hippocampal formation with a negative control and G3BP1 stain (both in green). Red boxes enclose the CA1/CA2 region shown in zoomed in images. **B)** Zoomed in scan image of area CA1/CA2 of the hippocampus (with DAPI co-stain in blue). Images were used to make qualitative comparisons. Lower DAPI intensity was noted in control samples. Scale bars: A=1000um; B=100um.
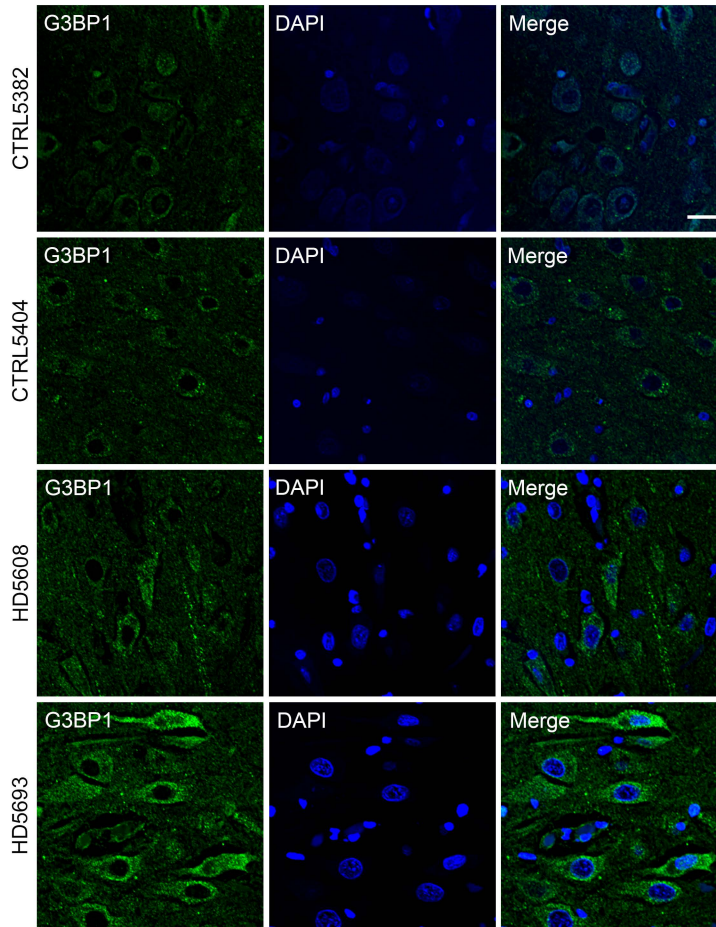
Supplemental Figure 10. G3BP1 immunoreactivity in the hippocampus of HD patients. G3BP1 immunofluorescence of the hippocampal formation of HD (grade 2) and control brains. Confocal images of hippocampal area CA1 depicting G3BP1-positive cells (in green). Images were used to make qualitative comparisons. Lower DAPI intensity was noted in control samples. Scale bar =20um.
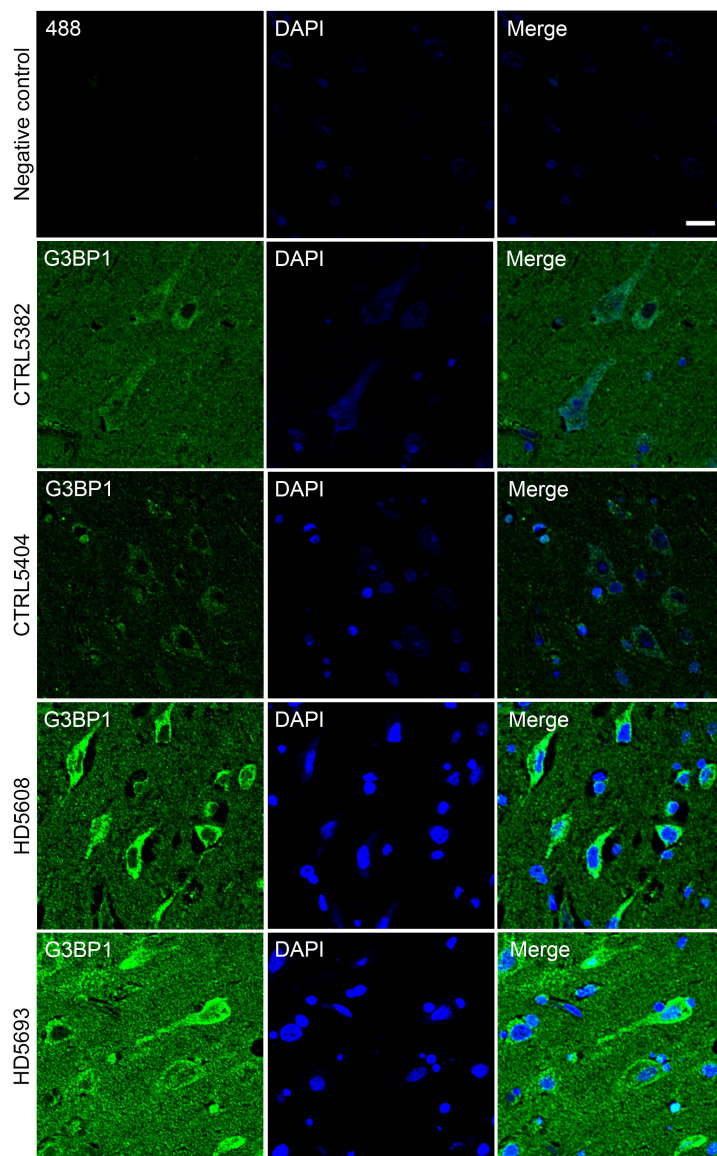
Supplemental Figure 11. G3BP1 immunoreactivity in the superior frontal cortex of HD patients. G3BP1 immunofluorescence (in green) of the superior frontal cortex of HD (grade 2) and control human brains. Images were used for qualitative comparisons. Lower DAPI intensity was noted in control samples.
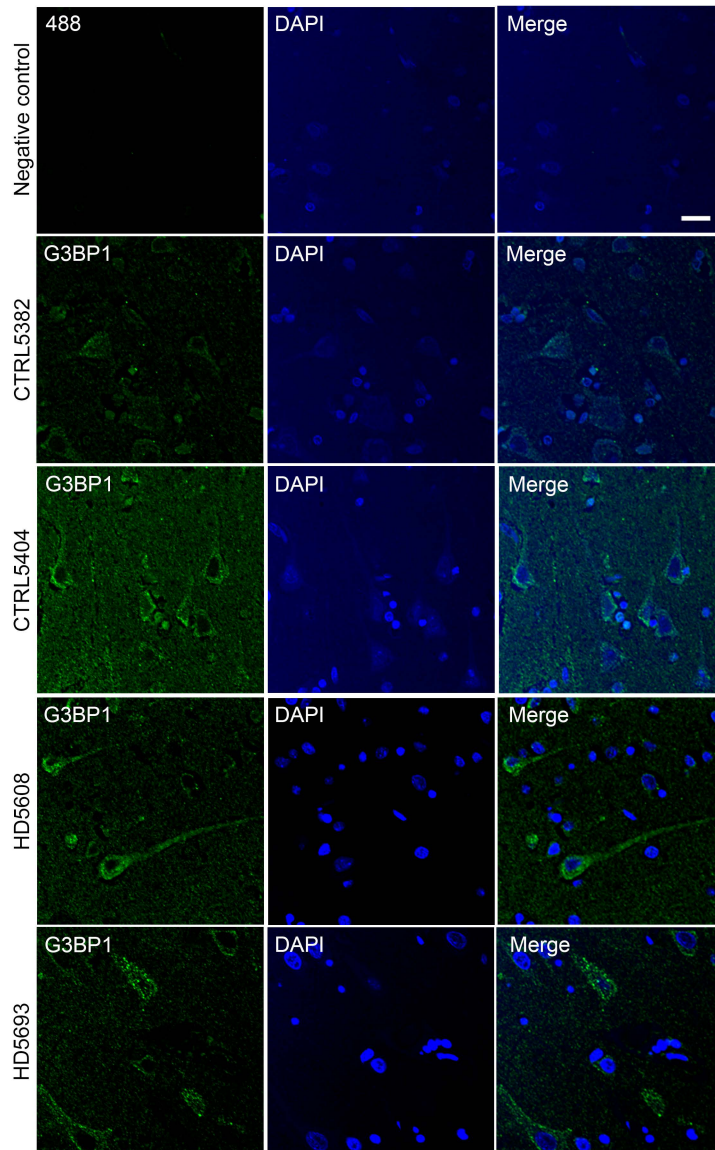
Supplemental Figure 12. G3BP1 immunoreactivity in the parietal cortex of HD patients. G3BP1 immunofluorescence (in green) of the parietal cortex of HD (grade 2) and control human brains. Images were used for qualitative comparisons. Lower DAPI intensity was noted in control samples. Scale bar=20um.
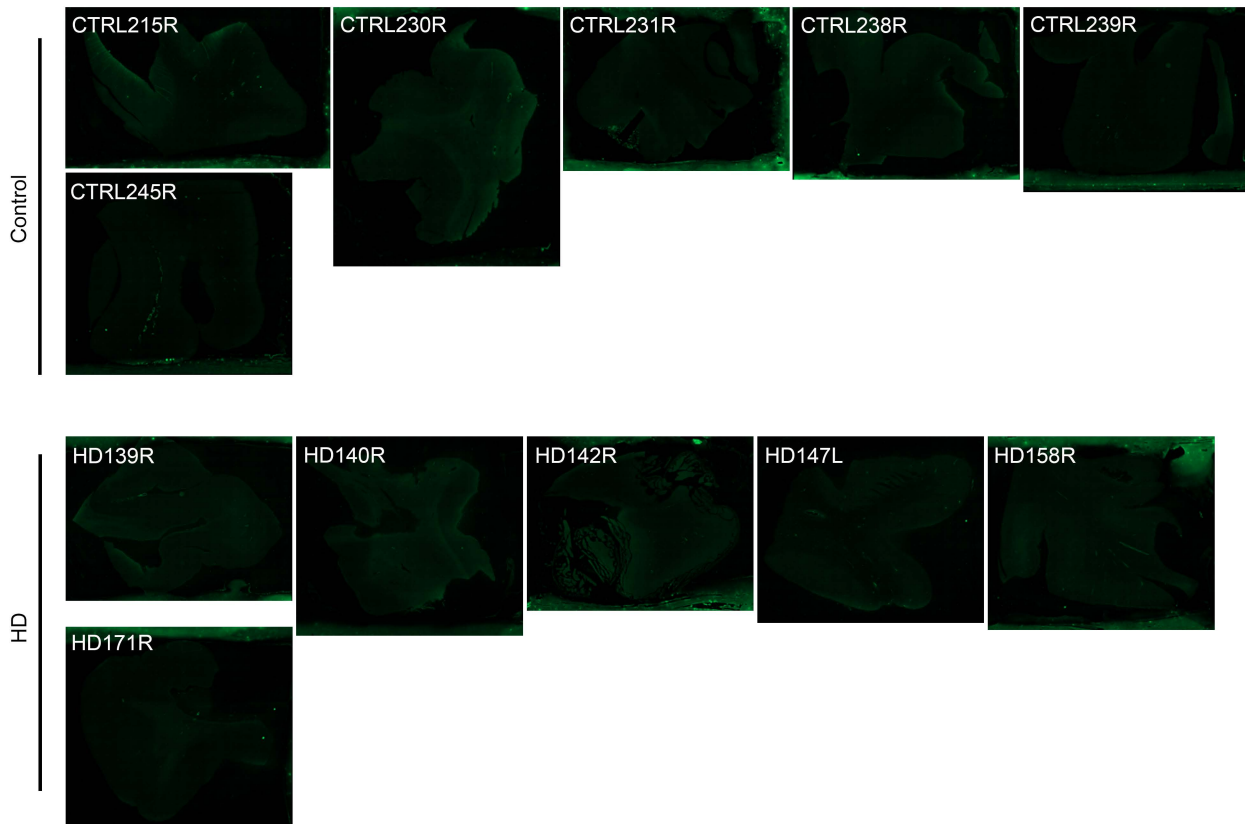
Supplemental Figure 13. Negative control immunostaining of superior frontal cortex blocks. Slide scanner images of postmortem superior frontal cortex blocks with negative control immunostaining (secondary antibody only, in green). Images represnt the background fluorescence present on blocks, and suggest relatively small background differences among samples.
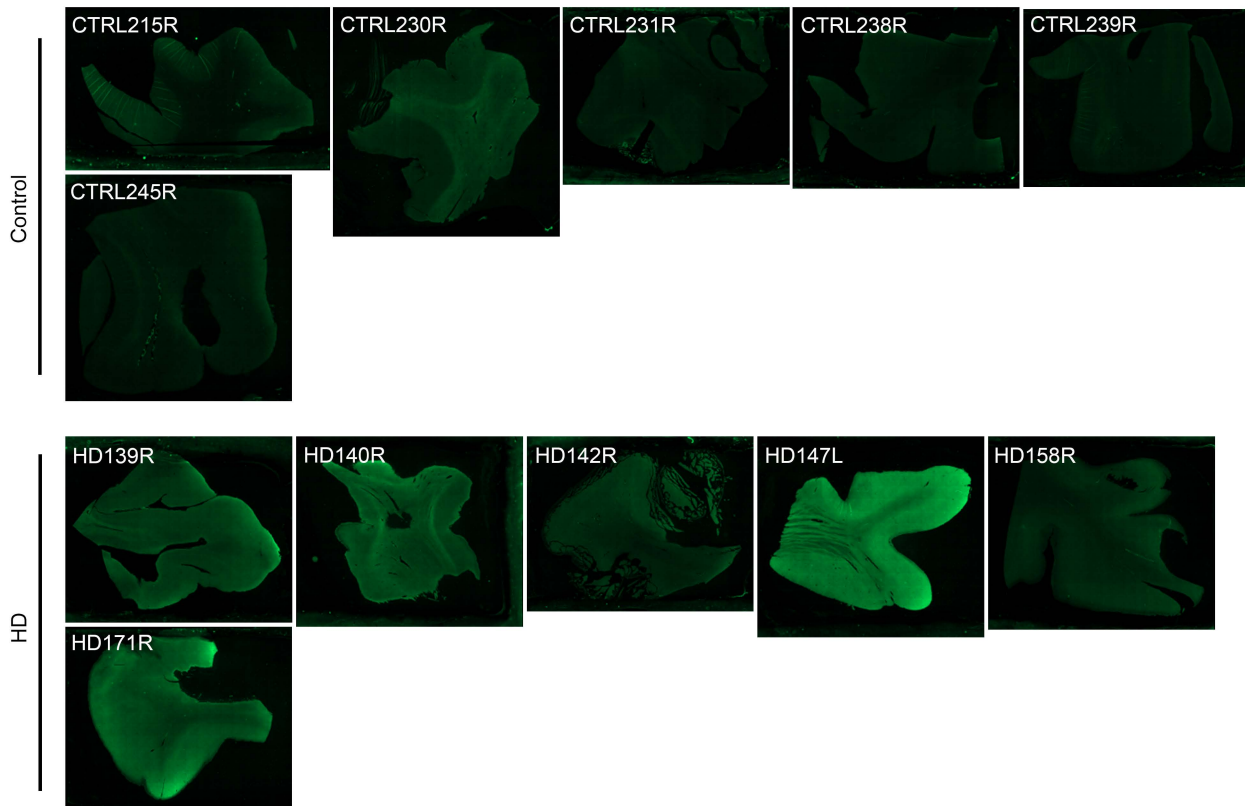
Supplemental Figure 14. G3BP1 immunostaining of superior frontal cortex blocks. Slide scanner images of postmortem superior frontal cortex blocks immunostained with G3BP1 (in green) and used to take high resolution confocal images of the cortical ribbon to quantitate G3BP1 SG densities.**.**
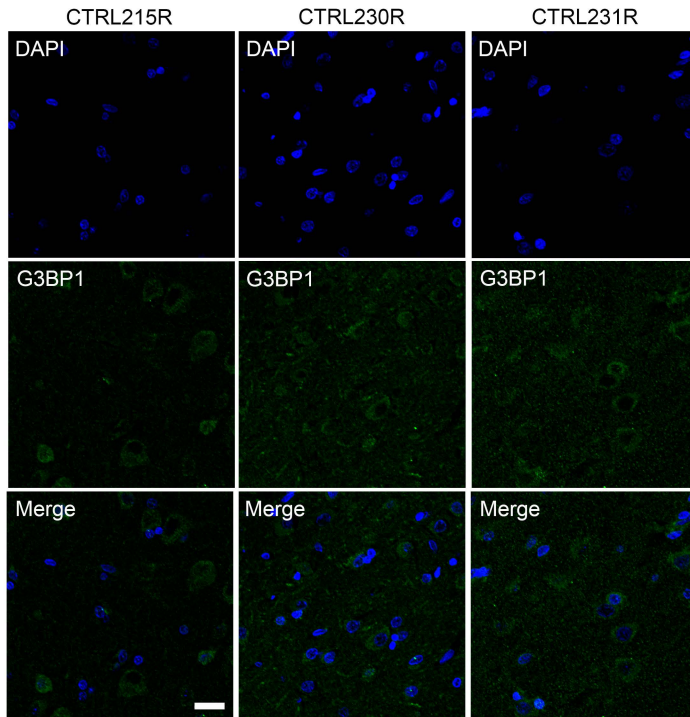
Supplemental Figure 15. Increased G3BP1 granule density in the superior frontal cortex of HD human brain (control samples). Panels for CTRL215R and CTRL231R are also presented in figure 7A (top two rows). Images were used to make quantitative G3BP1 SG density comparisons between HD and control samples. N= 6 HD; 6 Control. Scale bars:20um.
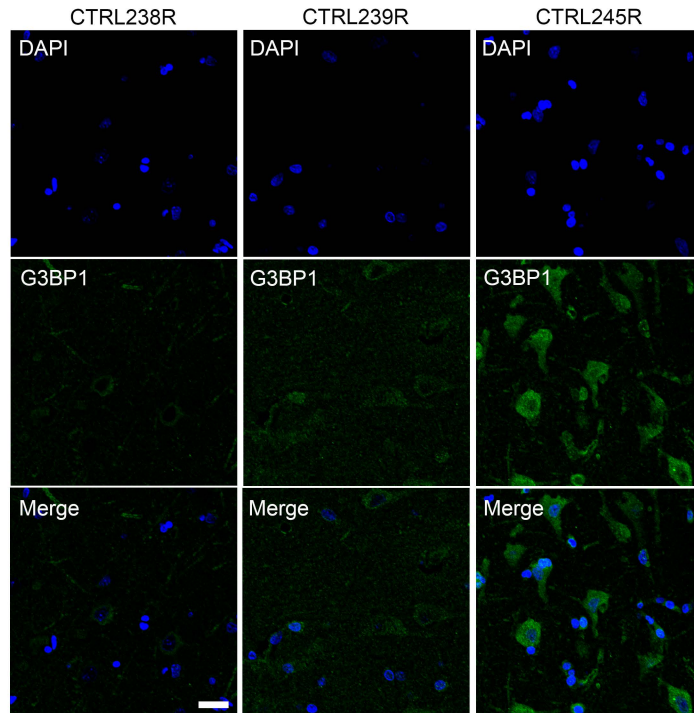
Supplemental Figure 15 (continued). Increased G3BP1 granule density in the superior frontal cortex of HD human brain (control samples). Images were used to make quantitative G3BP1 SG density comparisons between HD and control samples. N= 6 HD; 6 Control. Scale bars:20um.
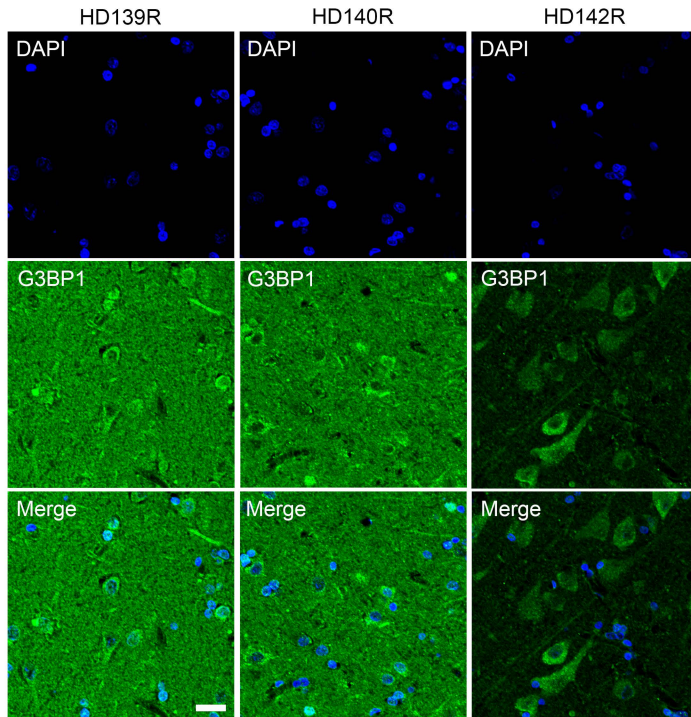
Supplemental Figure 15 (continued). Increased G3BP1 granule density in the superior frontal cortex of HD human brain (HD samples). Panels for HD139R and HD140R are also presented in figure 7A (bottom two rows). Images were used to make quantitative G3BP1 SG density comparisons between HD and control samples. N= 6 HD; 6 Control. Scale bars:20um.
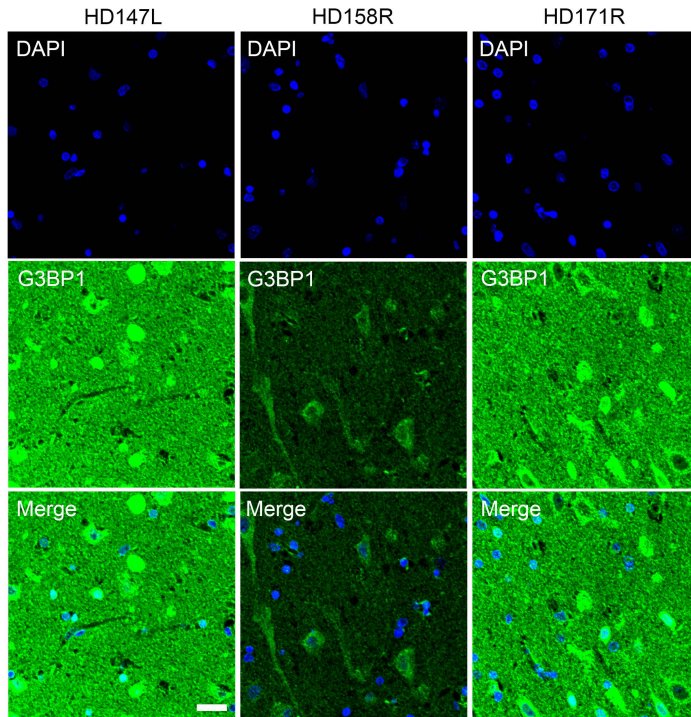
Supplemental Figure 15 (continued). Increased G3BP1 granule density in the superior frontal cortex of HD human brain (HD samples). Images were used to make quantitative G3BP1 SG density comparisons between HD and control samples. N= 6 HD; 6 Control. Scale bars:20um.
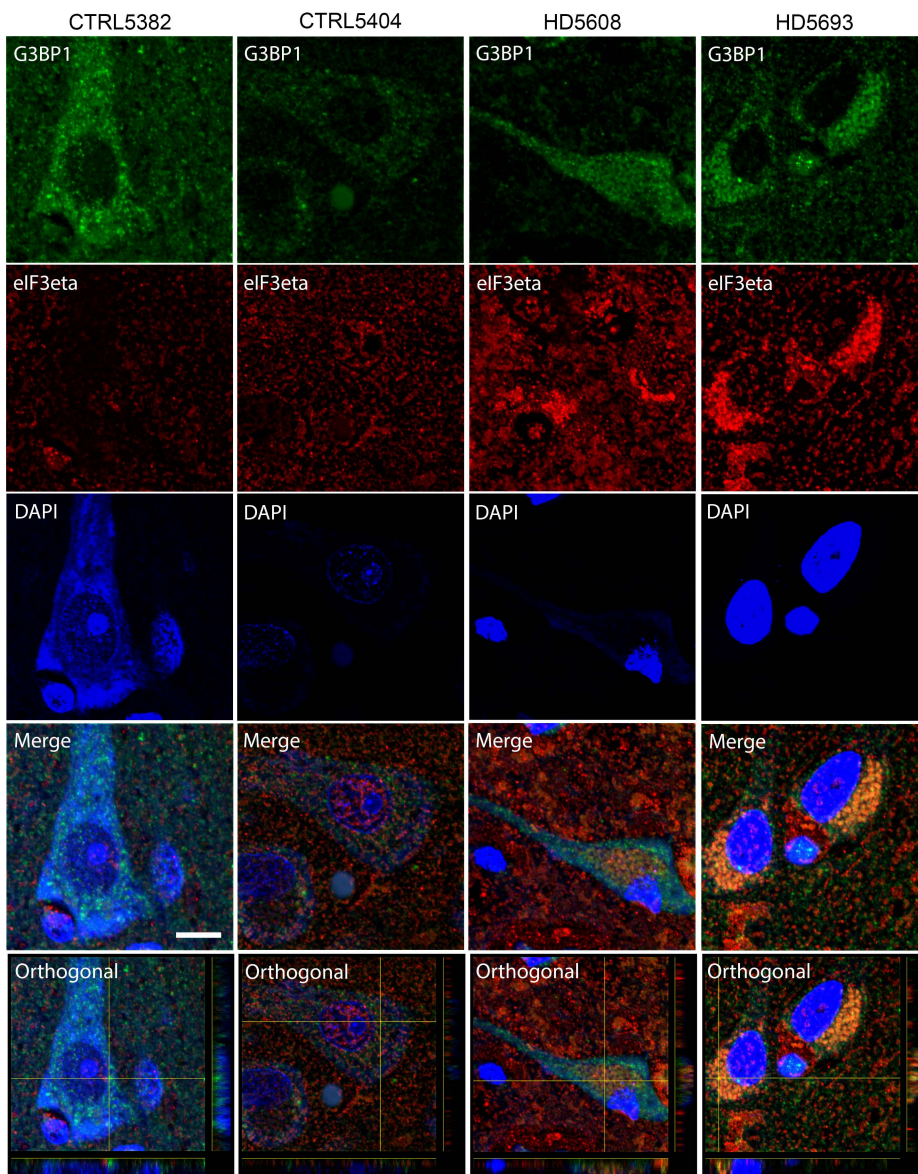
Supplemental Figure 16. G3BP1 granules colocalize with translation initiation factor eIF3eta in the superior frontal cortex of HD patients. Co-staining of SG markers G3BP1 (in green) and eIF3eta (in red) demonstrates colocalization in HD cases. Panels from figure 7C (CTRL5404 and HD5693) are presented again in this figure. Images were taken from 2 HD (grade 2) and 2 control cases. Orthogonal images show colocalization. Scale bar=10um**.**
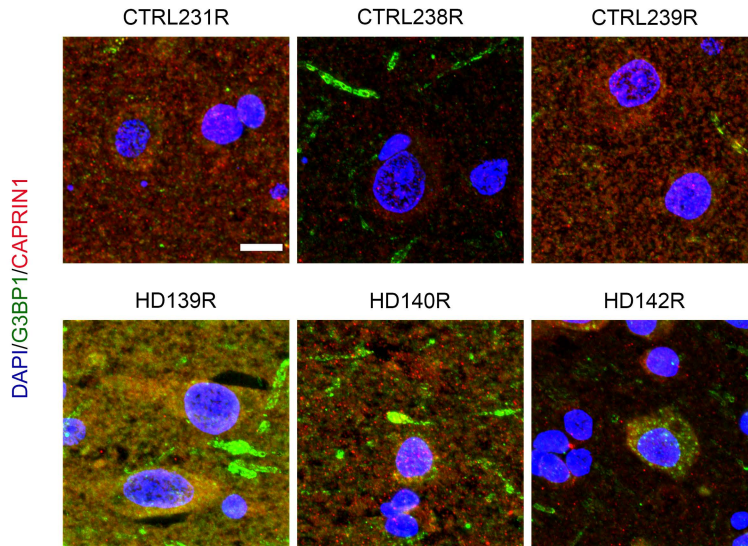
Supplemental Figure 17. Detection of SG-associated protein CAPRIN1 in the superior frontal cortex of HD human patients. The SG-associated RBP CAPRIN1 (in red) was detected in the parenchyma and cytoplasm of control and HD cortices. Of note, CAPRIN1 was detected in cells that are immunoreactive for G3BP1 (in green); however, we did not detect colocalization of CAPRIN1 and G3BP1 puncta. Scale bar=10um.

	miRNA	baseMean	log2FoldChange	lfcSE	stat	p-value	padj
Batch 1	hsa-miR-30e-5p	54.0066	-1.3356	0.429	-3.1134	0.00185	0.96335
	hsa-miR-1307-5p	6.06509	-6.1314	2.0375	-3.0093	0.00262	0.96335
	hsa-miR-449a	3.93847	4.8305	2.06734	2.33658	0.01946	0.96335
	hsa-let-7f-2-3p	3.49976	-5.3405	2.38671	-2.2376	0.02525	0.96335
	hsa-miR-584-5p	10.7835	-1.8939	0.87022	-2.1764	0.02953	0.96335
	hsa-miR-4634	7.04013	-5.1387	2.44135	-2.1048	0.03531	0.96335
	hsa-miR-381-3p	4.04843	4.09951	1.99834	2.05145	0.04022	0.96335
	hsa-miR-3907	6.15003	-6.12	3.03296	-2.0178	0.04361	0.96335
	hsa-miR-127-3p	5.29822	-3.2987	1.65742	-1.9903	0.04656	0.96335
	hsa-miR-29b-3p	28.6266	1.32361	0.66731	1.9835	0.04731	0.96335
Batch 2	hsa-miR-12136	3.57178	-2.2974	0.81625	-2.8146	0.00488	0.99845
	hsa-miR-6852-5p	1.05441	-3.4144	1.40459	-2.4309	0.01506	0.99845
	hsa-miR-4476	2.84722	-3.6436	1.51218	-2.4095	0.01597	0.99845
	hsa-miR-4750-3p	3.87093	-2.6797	1.14557	-2.3392	0.01933	0.99845
	hsa-miR-762	7.43113	1.07142	0.47626	2.24965	0.02447	0.99845
	hsa-miR-12126	3.54035	-2.962	1.43171	-2.0689	0.03856	0.99845
	hsa-miR-3675-3p	18.3645	0.92447	0.4521	2.04486	0.04087	0.99845
	hsa-miR-4725-3p	2.14193	1.95724	0.98018	1.99681	0.04585	0.99845
	hsa-miR-8069	16.2964	0.87203	0.43997	1.982	0.04748	0.99845
	hsa-miR-181c-3p	12.2489	-2.1381	1.08024	-1.9793	0.04778	0.99845
	hsa-miR-6785-5p	29.6265	0.90042	0.45688	1.97082	0.04874	0.99845
	hsa-miR-4687-3p	0.9087	2.64169	1.34676	1.96152	0.04982	0.99845

Supplemental Table 1. CSF EV miRNAs from HD vs. control differential expression analysis with p-values < 0.05, prior to correcting for multiple tests with the Benjamini-Hochberg method. N= 10 HD, 10 control. Sequencing studies were performed in two batches, following the same EV RNA isolation protocol.

miRNA	Total targets	Targets in HD PFC DEGs	Inverse direction	% overlap
hsa-miR-8076	2950	855	564	65.96
hsa-miR-3610	438	131	86	65.65
hsa-miR-624-5p	2078	646	421	65.17
hsa-miR-1243	3200	964	608	63.07
hsa-miR-146a-5p	283	74	46	62.16
hsa-miR-130b-5p	5727	1779	1100	61.83
hsa-miR-1322	2962	906	560	61.81
hsa-miR-181c-3p	1675	541	331	61.18
hsa-miR-4767	1203	391	238	60.87
hsa-miR-4442	644	188	109	57.98
hsa-miR-339-3p	729	283	164	57.95
hsa-miR-3125	5385	1666	965	57.92
hsa-miR-3917	710	214	123	57.48
hsa-miR-29b-3p	1265	426	244	57.28
hsa-miR-6846-3p	2673	880	500	56.82
hsa-miR-762	5621	1845	1046	56.69
hsa-miR-3679-3p	4906	1570	887	56.5
hsa-miR-6827-3p	2298	707	397	56.15
hsa-miR-4763-3p	6300	2050	1151	56.15
hsa-miR-6842-5p	4250	1412	786	55.67
hsa-miR-605-3p	4722	1486	823	55.38
hsa-miR-6782-5p	3452	1129	622	55.09
hsa-miR-3940-5p	3284	1033	561	54.31
hsa-miR-4700-5p	5553	1812	983	54.25
hsa-miR-6129	5364	1728	933	53.99
hsa-miR-6800-3p	3197	1014	540	53.25
hsa-miR-449a	754	256	136	53.13
hsa-miR-4535	2092	665	348	52.33
hsa-miR-3189-3p	4423	1397	730	52.25
hsa-miR-4634	638	196	102	52.04
hsa-miR-3127-5p	4249	1351	703	52.04
hsa-miR-4476	5956	1873	974	52
hsa-miR-6785-5p	7852	2509	1294	51.57
hsa-miR-7150	5077	1626	838	51.54
hsa-miR-2116-3p	4929	1572	810	51.53
hsa-miR-378b	223	72	37	51.39
hsa-miR-6840-3p	6772	2194	1126	51.32
hsa-miR-5589-5p	6349	2042	1043	51.08
hsa-miR-3158-3p	3263	1058	535	50.57
hsa-miR-4725-3p	5776	1816	918	50.55
hsa-miR-3944-5p	3815	1267	639	50.43

Supplemental Table 3. Filtered miRNAs from miRNA-mRNA overlap analysis.
List of 41 miRNAs that target DEGs in the prefrontal cortex (PFC) of HD patients. Because the expression level of a miRNA is negatively correlated to the expression level of its target gene, miRNAs whose expression levels were not the inverse of their target genes 50% or more of the time (% overlap) were filtered out.

	GO term	Fold enrichment	Raw p-value	FDR
Biological process	glutamate secretion (GO:0014047)	2.69	2.03E-03	4.86E-02
	embryonic forelimb morphogenesis (GO:0035115)	2.58	1.73E-03	4.30E-02
	forelimb morphogenesis (GO:0035136)	2.52	8.85E-04	2.47E-02
	positive regulation of sodium ion transport (GO:0010765)	2.51	2.08E-03	4.92E-02
	macrophage activation (GO:0042116)	2.46	3.37E-04	1.07E-02
	cellular extravasation (GO:0045123)	2.46	1.01E-03	2.76E-02
	regulation of sodium ion transmembrane transporter activity (GO:2000649)	2.41	2.82E-04	9.19E-03
	regulation of sodium ion transmembrane transport (GO:1902305)	2.31	1.82E-04	6.22E-03
	synaptic vesicle exocytosis (GO:0016079)	2.24	4.13E-04	1.27E-02
	regulation of myeloid leukocyte mediated immunity (GO:0002886)	2.24	1.24E-03	3.25E-02
Cellular component	presynaptic active zone membrane (GO:0048787)	2.6	2.32E-03	4.35E-02
	presynaptic active zone (GO:0048786)	2.15	3.89E-04	9.52E-03
	specific granule membrane (GO:0035579)	2.12	1.10E-04	3.30E-03
	tertiary granule (GO:0070820)	1.97	3.99E-06	1.57E-04
	tertiary granule membrane (GO:0070821)	1.97	2.17E-03	4.11E-02
	plasma membrane raft (GO:0044853)	1.92	3.69E-04	9.14E-03
	specific granule (GO:0042581)	1.87	4.35E-05	1.41E-03
	secretory granule membrane (GO:0030667)	1.82	7.67E-08	3.95E-06
	sarcolemma (GO:0042383)	1.79	4.39E-04	1.06E-02
	clathrin-coated vesicle membrane (GO:0030665)	1.79	1.77E-03	3.48E-02
Molecular function	DNA-binding transcription repressor activity, RNA polymerase II-specific (GO:0001227)	1.8	1.52E-06	2.30E-04
	DNA-binding transcription repressor activity (GO:0001217)	1.8	1.52E-06	2.23E-04
	DNA-binding transcription activator activity, RNA polymerase II-specific (GO:0001228)	1.6	7.94E-07	1.33E-04
	DNA-binding transcription activator activity (GO:0001216)	1.6	1.05E-06	1.69E-04
	RNA polymerase II regulatory region DNA binding (GO:0001012)	1.52	2.65E-09	1.13E-06
	RNA polymerase II proximal promoter sequence-specific DNA binding (GO:0000978)	1.51	1.73E-06	2.26E-04
	RNA polymerase II regulatory region sequence-specific DNA binding (GO:0000977)	1.51	5.73E-09	1.92E-06
	amide binding (GO:0033218)	1.5	1.70E-04	1.42E-02
	proximal promoter sequence-specific DNA binding (GO:0000987)	1.5	2.86E-06	3.44E-04
	transcription regulatory region sequence-specific DNA binding (GO:0000976)	1.49	7.38E-09	2.31E-06

Supplemental Table 4. Top 10 GO terms for biological process, cellular component, and molecular function, using the predicted gene targets of the final 41 filtered CSF EV miRNAs.

miRNA	logFC	p-value	FDR q-value
miR-10b-3p	1.45	2.13E-12	4.98E-10
miR-1298-3p	−0.78	5.52E-09	1.03E-06
miR-302a-3p	0.81	3.72E-06	4.98E-04
miR-223-3p	0.75	1.94E-05	1.82E-03
miR-3200-3p	−0.32	4.85E-05	4.14E-03
miR-302a-5p	0.7	5.70E-05	4.46E-03
miR-1264	−0.53	9.49E-05	6.36E-03
miR-6734-5p	−0.79	8.86E-05	6.36E-03
miR-144-5p	0.94	1.04E-04	6.53E-03
miR-138-2-3p	−0.38	1.43E-04	8.38E-03
miR-490-5p	−0.62	2.62E-04	1.04E-02
miR-5695	0.47	2.73E-04	1.04E-02
miR-885-5p	−0.35	2.77E-04	1.04E-02
miR-1298-5p	−0.81	3.84E-04	1.20E-02
miR-16-2-3p	0.71	3.98E-04	1.21E-02
miR-106a-5p	0.44	5.64E-04	1.43E-02
miR-142-5p	0.6	5.77E-04	1.43E-02
miR-549a	0.95	5.67E-04	1.43E-02
miR-5680	−0.35	9.93E-04	2.27E-02
miR-3065-5p	0.42	1.04E-03	2.33E-02
miR-4787-3p	−0.33	1.23E-03	2.62E-02
miR-101-5p	0.28	1.47E-03	2.88E-02
miR-483-5p	1.16	1.52E-03	2.91E-02
miR-1185-1-3p	−0.41	1.70E-03	3.12E-02
miR-129-5p	−0.35	1.95E-03	3.22E-02
miR-888-5p	0.56	1.91E-03	3.22E-02
miR-126-5p	0.29	2.46E-03	3.88E-02
miR-34c-5p	−0.64	2.48E-03	3.88E-02
miR-218-1-3p	0.35	2.53E-03	3.89E-02
miR-548n	0.52	3.14E-03	4.46E-02
miR-148a-5p	0.52	3.31E-03	4.57E-02
miR-29a-3p	0.23	3.46E-03	4.70E-02
miR-153-5p	0.37	3.78E-03	4.79E-02
miR-28-5p	0.27	3.75E-03	4.79E-02
miR-7-2-3p	0.27	3.78E-03	4.79E-02

Supplemental Table 5. Differentially expressed miRNAs in the prefrontal cortex of HD patients that are predicted to target G3BP1. Adapted from Hoss et al., 2015 (97) list of 75 miRNAs differentially expressed in HD prefrontal cortex (FDR q-value < 0.05), combined study.

miRCURY LNA miRNA mimic	QIAGEN Catalog #
Negative Control	#YM00479902-ADB
hsa-miR-6129	#YM00473318-ADB
hsa-miR-4725-3p	#YM00472882-ADB
hsa-miR-605-3p	#YM00470339-ADB
hsa-miR-4700-5p	#YM00472802-ADB
hsa-miR-449a	#YM00473262-ADB
hsa-miR-4476	#YM00472685-ADB
hsa-miR-1322	#YM00470309-ADB

Supplemental Table 6. miRCURY LNA miRNA mimics used in 293T cell transfection studies.

Antigen	Type	Dilution	Manufacturer
Anti-G3BP1	Rabbit Polyclonal	1:300 (FF- and PE-IF) 1:1000 (cell culture IF) 1:1000 (WB)	cat. #RN048PW, MBL
Anti-G3BP1	Mouse Monoclonal	1:200 (PE-IF)	cat. # 611126, BD Biosciences
Anti-G3BP2	Rabbit Polyclonal	1:200 (FF-IF)	cat. #ab86135, Abcam
Anti-hnRNPA2/B1	Mouse Monoclonal	1:250 (FF-IF) 1:100 (PE-IF) 1:1000 (WB)	cat. #sc-53531, Santa Cruz Biotech.
Anti-eIF3eta	Mouse Monoclonal	1:200 (PE-IF)	cat. #sc-137214, Santa Cruz Biotech.
Anti-TDP43	Rabbit Polyclonal	1:300 (PE-IF)	cat. #10782-2-AP, Proteintech
Anti-CAPRIN1	Mouse Monoclonal	1:300 (PE-IF)	cat. #66352-1-IG, ThermoFisher
Anti-DCP1	Rabbit Polyclonal	1:200 (PE-IF)	cat. #ab47811, Abcam
Anti-Huntingtin (EM48)	Mouse Monoclonal	1:200 (FF-IF)	cat. #MAB5374, Millipore
Anti-Polyglutamine (1C2)	Mouse Monoclonal	1:500 (FF-IF)	cat. #MAB1574, Millipore
Anti-Huntingtin (3B5H10)	Mouse Monoclonal	1:500 (FF-IF)	cat. #MABN821, Millipore
Anti-Huntingtin (5490)	Mouse Monoclonal	1:500 (FF-IF)	cat. #MAB5490, Millipore
Anti-CaMK2	Mouse Monoclonal	1:300 (PE-IF)	cat. #ab22609, Abcam
Anti-alpha-tubulin	Mouse Monoclonal	1:5000 (WB)	cat. #05-829, Sigma-Aldrich

Supplemental Table 7. List of primary antibodies used for tissue staining and western blotting.
FF= free floating, PE= paraffin embedded, IF= immunofluorescence, WB= western blotting.

Supplemental Methods

EV RNA isolation, library preparation, and next generation sequencing. All experiments were conducted by QIAGEN Genomic Services. RNA was isolated from 4mL CSF using the exoRNeasy Serum/Plasma Maxi Kit (cat. #77064, QIAGEN) per the manufacturer's instructions. The library preparation was performed using the QIAseq miRNA Library Kit (cat. #331505, QIAGEN). A total of 5ul total RNA was converted into miRNA NGS libraries. Adapters containing UMIs were ligated to the RNA and RNA converted to cDNA. The cDNA was amplified using PCR (22 cycles) and during the PCR indices were added. After PCR the samples were purified, and library preparation QC was performed using either Bioanalyzer 2100 (Agilent). Based on quality of the inserts and the concentration measurements, the libraries were pooled in equimolar ratios, quantified using qPCR and sequenced on a NextSeq500 sequencing instrument. Raw data was de-multiplexed and FASTQ files for each sample generated using the bcl2fastq software (Illumina inc.). FASTQ data were checked using the FastQC tool.

EV characterization by fluorescent nanoparticle tracking analysis. EVs were isolated from 600uL CSF using the exoEasy Maxi Kit (cat. #76064, Qiagen) according to the manufacturer's instructions. EVs were visualized and quantified using ExoGlow-NTA fluorescent labeling kit on an LM10 NanoSight instrument (cat. #EXONTA200A-1, SBI Systems Biosciences, Palo Alto, CA). Each sample was measured in triplicate, and videos of data collection were analyzed to give the mean, mode, and estimated concentration for each particle size.

293T cell transfection and SG induction experiments. 293T cells (ATCC cat. #ACS-4500) were plated onto six-well plates at a density of 1.0×10^6 cells/well for LNA miRNA mimic transfections. Transfection with HiPerFect (Qiagen cat. #301705) and respective microRNA cocktails was done 6 hours after plating (10ul/well HiPerFect, 5nM LNA cocktail working concentration). Complete media change and passaging were performed 24 and 48

hours after transfection, respectively. Each condition was done in triplicate and plated onto 1X PDL coated (1hr) Millicell EZ 4-well glass chamber slides (cat. #PEZGS0416) at a density of 3.0×10^5 cells per well. For SG induction, cells were stressed with 250μM sodium arsenite (Sigma-Aldrich cat. #1062771000) for 30 minutes at 37°C, followed by fixation with 4%PFA for 10 minutes. For immunofluorescence staining, cells were permeabilized for 10 minutes with 0.5% triton-X in 1X PBS, blocked with 5% normal donkey serum (cat. #017-000-121, Jackson Immuno Research Laboratories), incubated overnight with a G3BP1 primary antibody (**Supplemental Table 7**), 2 hours secondary (1:400, cat. #A-21202, ThermoFisher), and coverslips were mounted using Fluoromount-G (cat. #00-4958-02). For biochemistry experiments, cell pellets were sonicated with a buffer containing 10mM Tris (pH 7.4), 158 mM NaCl, 1mM ethylenediaminetetraacetic acid (EDTA) (pH 8), 0.1% sodium dodecyl sulfate (SDS), 1% Triton X-100, protease inhibitors (Pierce Protease Inhibitor Tablets, cat. #A32963, ThermoFisher), and phosphatase inhibitors (Phosphatase Inhibitor Cocktail 2, cat. #P5726; Phosphatase Inhibitor Cocktail 3, cat. #P0044). Protein concentration was determined using the Lowry protein assay. Invitrogen 4%–12% bis-tris mini gels were used for SDS-PAGE, proteins were transferred to a PVDF membrane and nonspecific proteins were blocked with 5% milk in TBS (Tris-buffered saline). The following primary antibodies were used (details in **Supplemental Table 7**): G3BP1, hnRNPA2/B1. Blot was imaged with the LI-COR Odyssey System and normalized to REVERT 700 Total Protein Stain (cat. # 926-11010, LI-COR).

293T-G3BP1-GFP microRNA mimic Incucyte S3 imaging. 293T-G3BP1-GFP cells, gifted by Dr. Yeo's laboratory, were plated onto a 12 well plate at a density of 1.0×10^5 cells/well. 24 hours post plating cells were transfected with HiPerFect (Qiagen cat. #301705) and respective microRNA cocktails (5ul/well HiPerFect, 5nM LNA cocktail working concentration). Immediately after transfection reagents are added, cells were place into the Incucyte S3 Live Cell Analysis System (Essenbioscience) for 3 hours of acclimatation prior to the first imaging timepoint (0). 4 images in different areas of each well were taken every hour for 36 hours with the 'Phase channel' and 'Green channel' (300ms exposure) at 20X. For analysis, the average GFP integrated intensity of the

image was normalized to the confluency area determined by the Incucyte analysis software. The mean of the 4 images represents the average GFP signal for each well, and each condition had 4 technical replicate wells.

R6/2 mice and tissue processing. Male R6/2 mice and NT littermates (Transgene non-carrier C57B16/CBA) were obtained from Jackson Laboratories at 5 weeks and aged to 8 or 12 weeks for SG immunofluorescence experiments. All mice were group housed on a 12/12-hr light/dark schedule with as libitum access to food and water. Mice were euthanized by Euthasol injection at 8 or 12 weeks, followed by transcardial perfusion with 1X PBS and 4% PFA, and decapitation. The whole brain was dissected for immunofluorescence experiments and drop fixed in 4% PFA for one hour, then cryoprotected in 30% sucrose, frozen, and serially sectioned into 40 um slices using a vibratome.

Free-floating immunofluorescence staining. Floating brain sections were washed in 3x5 minutes in 1X PBS and blocked for 1 hour at room temperature with 5% Normal Donkey Serum in 0.3% Triton X-100. Sections were incubated in primary antibody overnight at 40C in 5% Normal Donkey Serum (cat. #017-000-121, Jackson Immuno Research Laboratories) in 0.3% Triton X-100. The following primary antibodies were used (details in **Supplemental Table 7**): G3BP1, G3BP2, hnRNPA2/B1, EM48 (reacts with the first 256 amino acids from human huntingtin), 1C2 (reacts with homopolymeric glutamine stretches), 3B5H10 (reacts with human huntingtin N-terminal fragment of 171 amino acids), 5490 (reacts with huntingtin protein amino acids 115-129). Sections were then washed 3x5 minutes in 1X PBS, and incubated in secondary antibodies for 1 hour at room temperature in 1X PBS. Secondary antibodies were used as follows: Alexa Fluor 488 (1:400, cat. #A-21202, ThermoFisher), Alexa Fluor 555 (1:400, cat. #A-31570, ThermoFisher). Sections were washed 3x5 minutes in 1X PBS and incubated in DAPI for 10 minutes at room temperature. Sections were then washed 3x5 minutes in 1X PBS. Mounting was performed using Fluoromount-G (cat. #00-4958-02).

Paraffin-embedded immunofluorescence staining. Tissue sections were deparaffinized, rehydrated, and treated with 10mM sodium citrate for 30 minutes at 95°C. Sections were washed 2x5 minutes in 1X PBS and blocked for 1 hour at room temperature with 5% Normal Donkey Serum in 0.1% Triton X-100. Sections were incubated in primary antibody overnight at 4°C in 1% Normal Donkey Serum (cat. #017-000-121, Jackson Immuno Research Laboratories) in 0.1% Triton X-100. The following primary antibodies were used (details in **Supplemental Table 7**): G3BP1, CaMK2, eIF3eta, TDP43, CAPRIN1, DCP1a. Sections were then washed 3x5 minutes in 1X PBS and incubated in secondary antibodies for 1 hour at room temperature in 1X PBS. Secondary antibodies were used as follows: Alexa Fluor 488 (1:400, cat. #A-21202, ThermoFisher), Alexa Fluor 555 (1:400, cat. #A-31570, ThermoFisher). Sections were washed 3x5 minutes in 1X PBS, treated with TrueBlack® Lipofuscin Autofluorescence Quencher (cat. #23007, Biotium), washed 3x5 minutes in 1X PBS, and incubated in DAPI for 10 minutes at room temperature. Sections were then washed 3x5 minutes in 1X PBS, and cover slips were mounted using Fluoromount-G (cat. #00-4958-02).

Microscopy. Confocal images were acquired with an Olympus FLUOVIEW FV 3000 microscope and images were taken with 10X, 20X, 40X and 60X oil objectives. All brain scan images were done using a ZEISS Axio Scan.Z1 imaging system.

Supplemental Acknowledgments

Supplemental videos

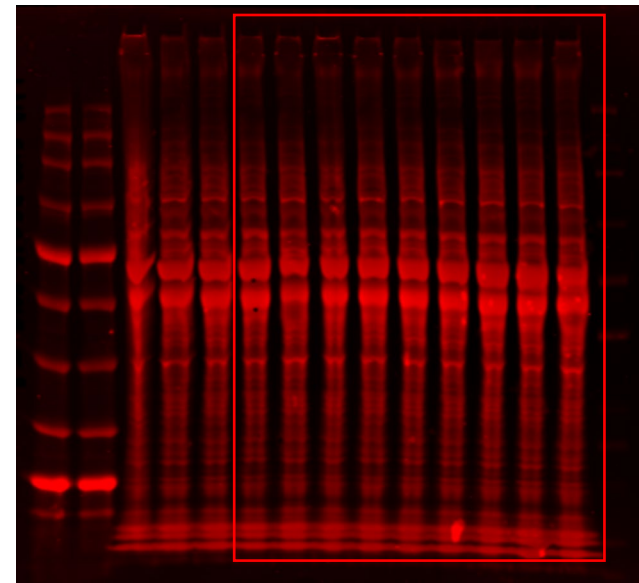Video 1: 88374-Sample#4_488T_20X_F_r02
Video 2: 88374-Sample#4_488T_20X_LS__r01
Video 3: 88374-Sample#7_488T_20X_F_r01
Video 4: 88374-Sample#7_488T_20X_LS_r01
Video 5: 88374-Sample#11_488T_20X_F__r01
Video 6: 88374-Sample#11_488T_20X_LS_r02
Video 7: 88374-Sample#51_488T_20X_F_r01
Video 8: 88374-Sample#51_488T_20X_LS_r02
Video 9: 88374-Sample#59_488T_20X_F_r02
Video 10: 88374-Sample#59_488T_20X_LS_r01
Video 11: 88374-Sample#60_488T_20X_F__r01
Video 12: 88374-Sample#60_488T_20X_LS_r01
Video 13: 88374-Sample#81_488T_20X_F_r01
Video 14: 88374-Sample#81_488T_20X_LS_r02
Video 15: 88374-Sample#82_488T_20X_F_r01
Video 16: 88374-Sample#82_488T_20X_LS_r01
Video 17: 88374-Sample#88_488T_20X_F_r02
Video 18: 88374-Sample#88_488T_20X_LS_r01
Video 19: 88374-Sample#102_488T_20X_F__r01
Video 20: 88374-Sample#102_488T_20X_F__r01

Full unedited gel for **Supplemental Figure 2**:

G3BP1

hnRNPA2/B1

Revert